

Oil spill classification based on satellite image using deep learning techniques

Abubakar Salihu Abba*, Noorfa Haszlinna Mustaffa, Siti Zaiton Mohd Hashim,
Razana Alwee

Faculty of Computing, University of Technology, Johor Bahru, Malaysia.

*Corresponding Author.

ICAC2023: The 4th International Conference on Applied Computing 2023.

Received 30/09/2023, Revised 10/02/2024, Accepted 12/02/2024, Published 25/02/2024



© 2022 The Author(s). Published by College of Science for Women, University of Baghdad.

This is an Open Access article distributed under the terms of the [Creative Commons Attribution 4.0 International License](https://creativecommons.org/licenses/by/4.0/), which permits unrestricted use, distribution, and reproduction in any medium, provided the original work is properly cited.

Abstract

An oil spill is a leakage of pipelines, vessels, oil rigs, or tankers that leads to the release of petroleum products into the marine environment or on land that happened naturally or due to human action, which resulted in severe damages and financial loss. Satellite imagery is one of the powerful tools currently utilized for capturing and getting vital information from the Earth's surface. But the complexity and the vast amount of data make it challenging and time-consuming for humans to process. However, with the advancement of deep learning techniques, the processes are now computerized for finding vital information using real-time satellite images. This paper applied three deep-learning algorithms for satellite image classification, including ResNet50, VGG19, and InceptionV4; They were trained and tested on an open-source satellite image dataset to analyze the algorithms' efficiency and performance and correlated the classification accuracy, precisions, recall, and f1-score. The result shows that InceptionV4 gives the best classification accuracy of 97% for cloudy, desert, green areas, and water, followed by VGG19 with approximately 96% and ResNet50 with 93%. The findings proved that the InceptionV4 algorithm is suitable for classifying oil spills and no spill with satellite images on a validated dataset.

Keywords: Classification, Marine, Oil spill, satellite images, deep learning.

Introduction

Oil and Gas products are generally transported by pipelines across a thousand kilometers worldwide. To provide reliable, secure, and dependent transportation of the products from one production depot to distribution depot, the pipeline was constructed to resist many environmental factors that lead to corrosion or leakages¹. In oil and gas companies, numerous issues and irregularities may cause severe damage to the connected oil and gas pipelines, which could eventually harm people, aquatic animals, and the environment that can cause

financial loss. Rusting and leakage are just a few abnormalities that might occur, leading to a severe problem, especially with offshore pipelines. Detecting a small leakage in any pipeline, be it a water pipe or an oil and gas pipe, is a crucial and pervasive challenge in any company that deals with conduit. Many companies have so much depended on the traditional techniques or use of some devices for surveillance of leakages. But, with the new advancements in science and technology, they come with an economical, safest, and simple method for

implementation². The use of remote sensing has been extremely helpful in monitoring adjustments, whether in climate or surface area, thereby saving time, money, and effort³.

One of the significant marine contaminants is oil spill pollution which seriously harms marine ecology⁴. Hence, timely identification of the leakage area is essential to prevent any serious issues that may arise⁵. Additionally, the effects of pipeline leakages escalate with the size of the leakage point; hence, leakages need to be identified quickly to stop them from spreading all over the surface. Implementing accurate and timely monitoring and detection systems for pipelines is necessary for minimizing the leak's effect.

The release of oil and gas into the natural environment due to human activities, intentionally or unintentionally, is called an oil spill. The most dangerous spill is a maritime spill, which is more risky than those spills on land or forest due to the fastest spreading all over the ocean and putting the

life of aquatic animals in danger⁶. So, there is a need for real-time detection of leakage points to prevent a severe problem that may develop⁷. The study of⁸ and⁹ made some observations for enhancing pipeline detection systems by employing the global potentiality of machine learning ML and deep learning DL methods.

Using deep learning based on the potential of artificial intelligence plays a vital role in providing an accurate detection result after carefully monitoring the situations¹⁰. ML techniques help to create a general model that can classify newly discovered data with little or no error due to its high computational power. ML algorithms are considered potent artificial intelligence technology that enables advanced systems for analytics to identify patterns in a billion bytes of data and develop dependable detection models. These models were built, tested, and validated based on a specific dataset in different scenarios to provide a maximum accurate result¹¹.

Related Work

Currently, numerous techniques are used in identifying and locating leakage points, including statistical techniques, traditional ML techniques, and semantic DL segmentation. Still, the techniques have some setbacks in detection accuracy, which is the most fundamental attribute^{12, 13} applied VGG16 using mask R-CNN with the in-house generated dataset called Nafta 2019 in detection and instance segmentation in oil spills using deep neural network and obtained an accuracy of 93%, which is not enough to depend on.¹⁴ applied deep convolutional neural network in detecting oil spillage from synthetic aperture radar SAR images with patches, but only obtained 94.01%, 83.51%, and 85.70% of accuracy, recall, and precision, respectively. But, the method did not consider pixel level, and there is a need to test the technique on an extensive dataset.¹⁵ applied YOLOv3 with a darknet-53 network in detecting leaks from underwater pipelines and achieved an accuracy of 93.67% and 77.05% of pipeline identification and leak point identification, respectively. But YOLO family algorithms are better at detecting moving objects; also, the images used were collected from a robot in the seabed.

The recent development of satellite sensors has significantly improved image processing, allowing the acquisition of images and processing them using computer vision algorithms. Furthermore, this enables the detection of actual leakage points in an offshore pipeline. As a result of these developments, quite several scholars have developed several kinds of algorithms for the detection of pipeline leakages, such as segmentation of threshold¹⁶, detection of edge¹⁷, and segmentation of zone¹⁸. Several efforts are currently going on to employ artificial intelligence to detect pipeline leakages resulting in oil spills.

The work of¹⁹ applied a convolutional neural network to monitor the offshore pipelines with the help of an in-house dataset generated from web mining and only achieved an accuracy of 92% which need further improvement with a valid dataset.²⁰ applied random forest in mapping a terrestrial oil spill using a satellite with sentinel-1 and sentinel-2 images and obtained a slight increase in accuracy to 95%. However, the identification of polluted areas is less accurate than detection. However, the technique is only applicable to a specified location.²¹ applied UNet-CNN in the

classification of oil spills with SAR images and obtained a slight increase in mIoU value to 75.70%.²² applied 23-layer CNN with sentinel-1 data obtained from the European space agency and achieved an accuracy of 92%, but the technique did not consider the segmentation of patches that measure the intensity of the spill.²³ applied AlexNet with GF-2 and RADARSAT-2 SAR images and compared them with the Support vector machine, Fuzzy C mean Clustering (FCM), and OTSU, but the AlexNet achieved a high identification accuracy.²⁴ applied V-Net with image flipping and rotation due to the scarcity of a large dataset and only achieved an accuracy of 90.65%. However, all the above methodologies have their shortcomings, starting from delays in response time, accuracy, and detection not in real-time. The work of²⁵ used traditional convolutional neural networks, which include support vector machine, random forest, and K-nearest neighbour as machine learning classifiers to automatically label the hyperspectral images dataset for classification of spill from satellite images; the CNN has a global perspective in terms of its ability to perform object classification and recognition²⁶. However, the

Materials and Methods

The methodology starts by collecting the data; the dataset used is Satellite Remote Sensing Image RSI-CB256, an open source obtained from Kaggle.com; It is a satellite image classification with four (4) different categories combined from a sensor and Google map snapshot that contains about 5631 images with a size of 256 x 256 pixels from 4 categories named water with 1500 images, cloudy with 1500 images, green area with 1500 images, and desert with 1131 images. The interpretation of images obtained from remote sensing and its vast

classifiers achieved better accuracy in a specified region (Gulf of Mexico) selected for the research. However, there is no guarantee that the proposed method will perform better when applied in different areas.²⁷ Proposed decision tree forest DTF method for classifying an oil spill and look alike using SAR images dataset for the evaluation. However, the method is based on the data's geometrical, textual, and physical features at present; the result shows that combining more features increases the classification accuracy. So, there is a need to separate the features and test the method on large datasets for verification. In summary, from the reviewed work, most of the proposed techniques depend heavily on the region of interest and the availability of data for that region. Therefore, in this paper, an oil spill classification image dataset available for research will be utilized using the most potent deep-learning classification algorithms²⁸. ResNet, VGG, and Inception series are among the best classification algorithms that achieved good performance based on satellite image datasets, as demonstrated in the work of²⁹.

applications have substantially advanced over the past decade. Since RS images are increasingly becoming more easily available now, there is a need to increase their automated interpretation. The dataset is necessary for developing and evaluating the interpretation model in this scenario. After collecting the data, the dataset was separated into 70% training and 30% validation sets of 3941 and 1690, respectively. However, the images were augmented and scaled into the target size of 224, 224 in 3 dimensions, as shown in Fig. 1.

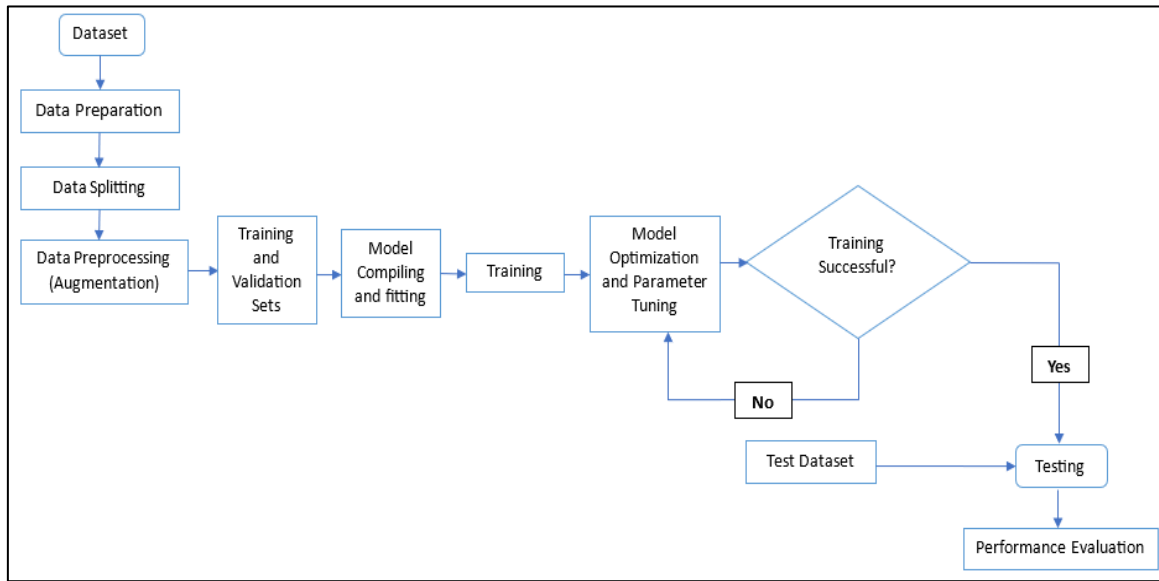


Figure 1. Methodology flowchart

The next step is data preprocessing, thereby augmenting the data by changing the orientation and resizing the image to a square shape to have the exact image dimensions; Applying geometrics transformations to images like vertical or horizontal flipping, cropping of images, rotation of images, and noise injection will help the model to understand different image orientation and position of an object on the image. The last stage of data preprocessing is to label each image, making it easy for the model to learn quickly for each given input.

The next phase is the model summary for InceptionV4, ResNet50, and VGG19, which helps in understanding the architectural structure of the CNN model that has been made, as shown in Fig. 2, Fig. 3, and Fig. 4.

Fig. 2 shows the summary of the architectural model of InceptionV4 within ten epochs, having several activations after convolutional layers and only one dropout layer, the architectural summary of the model produces the accuracy and loss value presented in Fig. 7.

```

Model: "Inception-V4"
=====
Layer (type)                Output Shape          Param #   Connected to
-----
input_1 (InputLayer)        [(None, 224, 224, 3  0
                           )]
conv2d (Conv2D)             (None, 111, 111, 32  896
                           )
batch_normalization (BatchNorm
alization)                  (None, 111, 111, 32  128
                           )
activation (Activation)     (None, 111, 111, 32  0
                           )
conv2d_1 (Conv2D)           (None, 109, 109, 32  9248
                           )
batch_normalization_1 (BatchNo
rmalization)                (None, 109, 109, 32  128
                           )
activation_1 (Activation)   (None, 109, 109, 32  0
                           )
...
Total params: 52,285,668
Trainable params: 52,222,436
Non-trainable params: 63,232
    
```

Figure 2. InceptionV4 model summary

The model architecture of InceptionV4, as shown in Fig. 2, is formed from the combination of Inception and ResNet-v2; these residual connections allow better training of deeper networks by mitigating the vanishing gradient problem. Combining Inception-style modules and residual connections makes InceptionV4 more robust to overfitting and allows it to learn complex patterns and features in the data effectively. Fig. 3 shows the summary of the

architectural model of ResNet50, which utilized the bottleneck approach to have lower parameters and multiplications of a matrix for faster training. But reducing the multiplication matrix also reduces the accuracy of this model, as shown in Fig. 5. However, ResNet50 has less efficient and straightforward architecture when compared with InceptionV4.

```

Model: "model"
-----
Layer (type)                Output Shape          Param #   Connected to
-----
input_1 (InputLayer)        [(None, 224, 224, 3  0
)]
conv1_pad (ZeroPadding2D)   (None, 230, 230, 3)  0         ['input_1[0][0]']
conv1_conv (Conv2D)         (None, 112, 112, 64  9472      ['conv1_pad[0][0]']
)
conv1_bn (BatchNormalization) (None, 112, 112, 64  256       ['conv1_conv[0][0]']
)
conv1_relu (Activation)     (None, 112, 112, 64  0         ['conv1_bn[0][0]']
)
pool1_pad (ZeroPadding2D)   (None, 114, 114, 64  0         ['conv1_relu[0][0]']
)
pool1_pool (MaxPooling2D)   (None, 56, 56, 64)  0         ['pool1_pad[0][0]']
...
Total params: 26,747,780
Trainable params: 26,690,564
Non-trainable params: 57,216
    
```

Figure 3. ResNet50 model summary

Fig. 4 displays the summary of the architectural model of VGG19, consisting of several convolutional layers assembled on top of each other, thereby making it more expensive in

computation and prone to overfitting when dealing with limited data, and it's a relatively simple and deep architecture with single activation layer compared with InceptionV4.

Layer (type)	Output Shape	Param #
input_2 (InputLayer)	[(None, 224, 224, 3)]	0
block1_conv1 (Conv2D)	(None, 224, 224, 64)	1792
block1_conv2 (Conv2D)	(None, 224, 224, 64)	36928
block1_pool (MaxPooling2D)	(None, 112, 112, 64)	0
block2_conv1 (Conv2D)	(None, 112, 112, 128)	73856
block2_conv2 (Conv2D)	(None, 112, 112, 128)	147584
block2_pool (MaxPooling2D)	(None, 56, 56, 128)	0
block3_conv1 (Conv2D)	(None, 56, 56, 256)	295168
block3_conv2 (Conv2D)	(None, 56, 56, 256)	590080
block3_conv3 (Conv2D)	(None, 56, 56, 256)	590080
block3_conv4 (Conv2D)	(None, 56, 56, 256)	590080
...		
Total params: 21,611,588		
Trainable params: 1,583,108		
Non-trainable params: 20,028,480		

Figure 4. VGG19 model summary

The next phase is compiling and fitting the model, where the optimization and loss are applied in training to get model results that can classify the imputed images. Therefore, after the compilation of the model phase, the next is model training, which enables the model to read all the parameters, including the number of epochs for getting the loss, accuracy, loss validation value, and accuracy validation value.

Lastly, the model evaluation is based on an evaluation generator. It calculates overall metrics like accuracy, precision, recall, and f1-score. These metrics give a detailed view of the model's performance.

Parameter Settings

During the training of the convolutional neural network, error measurement is required for computing the expected outputs and the training

output, which requires an optimization algorithm for that. Adam optimizer³⁰ was considered in this research, and Amsgrad = True, as shown in Table 1. The choice of learning rate is vital; it can affect any CNN algorithm's prediction accuracy, time, and computational cost. So here, a 0.00001 learning rate was considered due to the dataset and the model used to have an optimal result.

Table 1. Hyperparameter settings for CNN Models

Parameters	Settings
Epochs	10
Target size	224, 224
Batch size	32
Output classes	4
Adam Optimizer	
Learning Rate (lr)	0.00001
beta_1	0.6
Beta_2	0.9
Amsgrad	True

Results and Discussion

During the experiment, three models were implemented, which include ResNet50, VGG19, and InceptionV4. Each model has been trained and tested with the dataset in the same environment and

settings to find the best among them for classifying satellite images, as shown in Fig. 2, Fig. 3, and Fig. 4.

Model result and accuracy on ResNet50

From the ResNet50 model architecture, as shown in Fig. 3, after ten epochs with a batch size of 32 based on the image shape of 224,224,3 using the training sample of 3941 images while the validation has 2690 images, the model was able to achieve overall accuracy of 91% with 61% loss.

Tables 2 and 3 show the result of the overall metrics for accuracy, precision, recall, and f1-score for each dataset class.

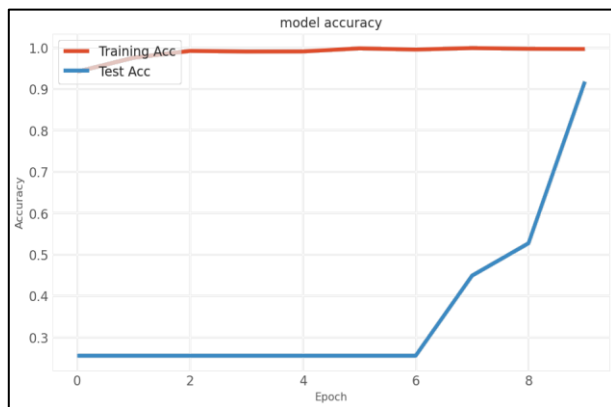
Table 2. Overall metrics for ResNet50

Metrics	Values
Accuracy	0.9183431952662722
Precisions	0.9375075473976572
Recall	0.9183431952662722
F1-Score	0.9179678866226003

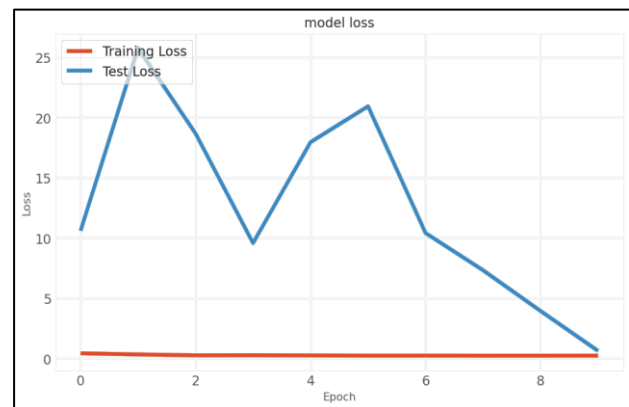
Table 3. Metrics per class

Metrics	Precisions	Recalls	F1-Scores	Support
Cloudy	1.00	0.98	0.99	450
Desert	1.00	0.98	0.99	340
Green area	1.00	0.73	0.84	450
Water	0.77	1.00	0.87	450
Accuracy			0.92	1690
Macro-Avg	0.94	0.92	0.92	1690
Weighted Avg	0.94	0.92	0.92	1690
Cloudy	1.00	0.98	0.99	450

The result of ResNet50, shown in Fig. 5, achieved the least accuracy due to the use of the bottleneck approach utilized by the model. The model has an overfitting problem that needs more residual connections in the architecture to solve it.



(a)



(b)

Figure 5. ResNet50 model curve (a) accuracy (b) loss

Model result and accuracy on VGG19

The VGG19 model architecture, as shown in Fig.4, produces the model curve accuracy and model curve loss displayed in Fig. 6, and the result of the overall metrics for each dataset class was also shown in Tables 4 and 5 with an accuracy of 96% and loss of 23%.

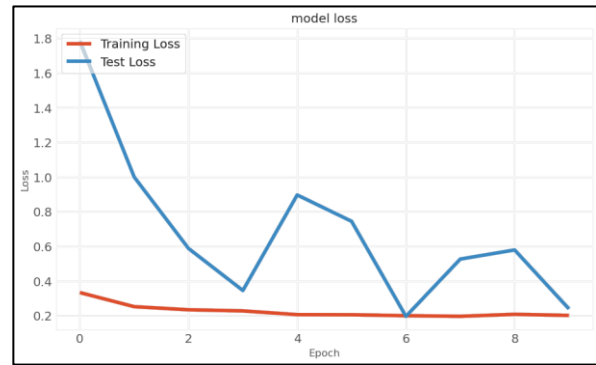
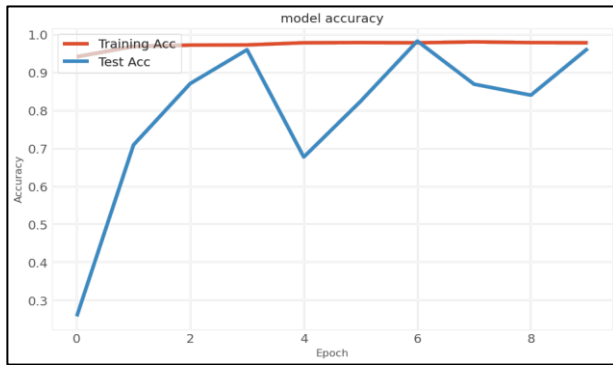
Table 4. Overall metrics for VGG19

Metrics	Values
Accuracy	0.9627218934911242
Precisions	0.9664300446542559
Recall	0.9627218934911242
F1-Score	0.9628361681335859

Table 5. Metrics per class

Metrics	Precisions	Recalls	F1-Scores	Support
Cloudy	1.00	0.98	0.99	450
Desert	1.00	1.00	1.00	340
Green area	0.99	0.88	0.94	450
Water	0.88	0.99	0.94	450
Accuracy			0.96	1690
Macro-Avg	0.97	0.96	0.97	1690
Weighted Avg	0.97	0.96	0.96	1690
Cloudy	1.00	0.98	0.99	450

Fig. 6 shows a good result of VGG19. However, the model suffered from overfitting, which needs more dense layers and dropouts to make it more efficient.



(a) (b)
Figure 6. VGG19 model curve (a) accuracy (b) loss

Model Result and accuracy on InceptionV4

The InceptionV4 architecture from Fig. 2 produces the best result compared to VGG19 and ResNet50 on the same dataset and the environment. Tables 6 and 7 show the model's overall accuracy for all the dataset classes, with an accuracy of 97% and only a loss of 10%.

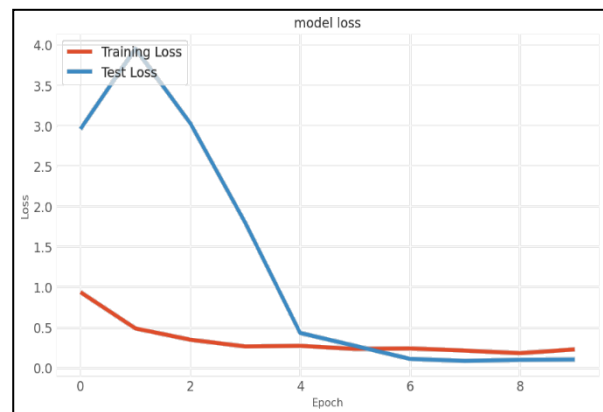
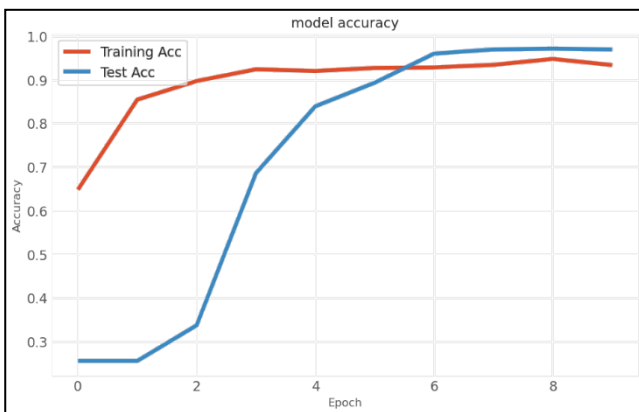
Table 6. Overall metrics for InceptionV4

Metrics	Values
Accuracy	0.9698224852071006
Precisions	0.9698858240086438
Recall	0.9698224852071006
F1-Score	0.9698272076868117

Table 7. Metrics per class

Metrics	Precisions	Recalls	F1-Scores	Support
Cloudy	0.97	0.98	0.97	450
Desert	0.98	0.98	0.98	340
Green area	0.98	0.96	0.97	450
Water	0.96	0.97	0.96	450
Accuracy			0.97	1690
Macro-Avg	0.97	0.97	0.97	1690
Weighted Avg	0.97	0.97	0.97	1690
Cloudy	0.97	0.98	0.97	450

Fig. 7 demonstrates the potentiality of the InceptionV4 model against existing CNN models on the classification of images.



(a) (b)
Figure 7. InceptionV4 model curve (a) Accuracy (b) Loss

Overall, InceptionV4 is a state-of-the-art architecture combining the best ideas from Inception and ResNet family, providing a more efficient and robust model than VGG19 and

ResNet50. It can handle more complex tasks and datasets, achieving higher accuracy and faster training convergence. However, choosing the best

model depends on the specific use case and available resources.

CNN Models comparison and accuracy

The result obtained by InceptionV4 in this study performed better when compared with ³¹, with an

increase of 13% accuracy. However, both ResNet50 and VGG19 models used in this study achieved better results than ³².

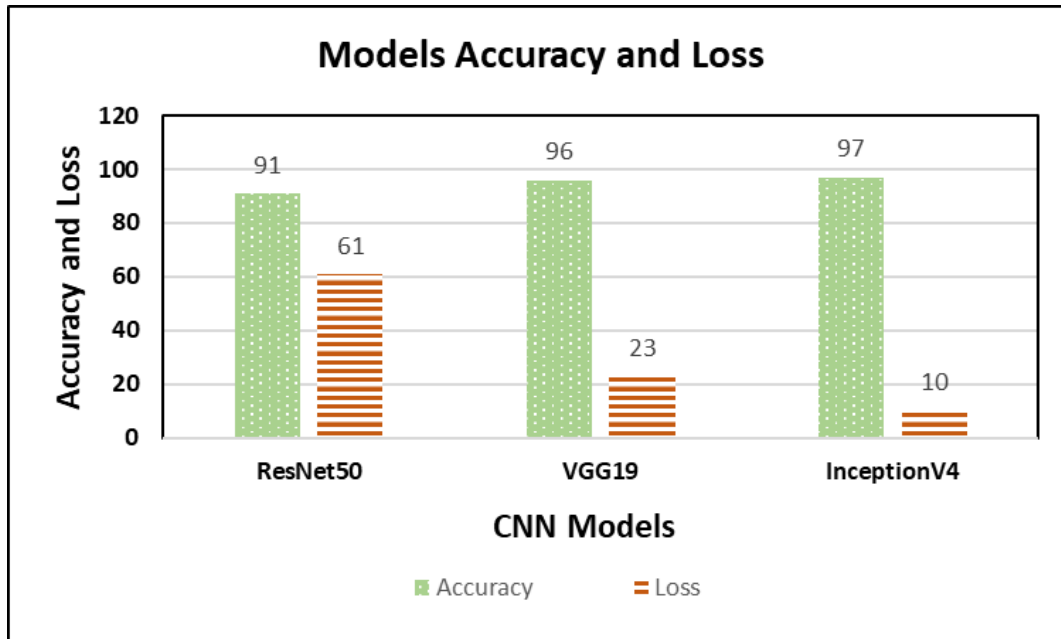


Figure 8. CNN Models comparison and accuracy

Fig. 8 shows the results of the comparisons of three CNN based on accuracy and loss; the result proved that InceptionV4 is the best in this research with the highest accuracy and lowest loss value due to the

utilization of several activation functions, which shows how well the model is performing in prediction by having the highest accuracy and the low loss value.

Conclusion

In conclusion, after implementing the three models, the results show that the InceptionV4 model performed better in classifying satellite images based on the input data regarding the accuracy, precisions, recall, and f1-score for all dataset classes with 97% across all the metrics and only 10% loss during testing, ResNet50 achieved 91% accuracy with 61% loss, and VGG19 achieved 96% accuracy with 23% loss. However, due to InceptionV4 efficiency, the model performs significantly in classification and learning rate compared to ResNet50 and VGG19 models on a commonly used training and testing ratio of 70% and 30%.

However, like other deep learning models, the better accuracy of InceptionV4 can be ascribed to its ability to effectively capture complex features, optimize the training process with residual connections, and lower overfitting problems. Therefore, Combining Inception-style modules with residual connections allows InceptionV4 to balance depth and width well, making it more efficient and robust than VGG19 and ResNet50. The model's performance will be investigated in future work on a large available public satellite image dataset with multi-class labels.

Acknowledgment

This research was supported by the Minister of Higher Education under the Fundamental Research Grant Scheme (FRGS/1/2021/ICT02/UTM/02/13)

Authors' Declaration

- Conflicts of Interest: None.
- We hereby confirm that all the Figures and Tables in the manuscript are ours. Besides, the Figures and images, which are not ours, have been given the permission for re-publication attached with the manuscript.
- Ethical Clearance: The project was approved by the local ethical committee in University of Technology Malaysia (UTM)-skudai, Johor Bahru Malaysia.

Authors' Contribution Statement

M.N.H. conducted the literature review and data acquisition, A.A.S. performed the analysis and interpretation of the result, A.R. drafted the manuscript with input from all authors, and

H.S.Z.M. reviewed the final version of the manuscript and performed editing and proofreading. All authors discussed the results and contributed to the final manuscript.

References

1. Adegboye MA, Fung WK, Karnik A. Recent advances in pipeline monitoring and oil leakage detection technologies: Principles and approaches. *Sensors (Switzerland): MDPI AG.* 2019. <https://doi.org/10.3390/s19112548>.
2. Aljameel SS, Alomari DM, Alismail S, Khawaher F, Alkudhair AA, Aljubran F, et al. An Anomaly Detection Model for Oil and Gas Pipelines Using Machine Learning. *Computation.* 2022;10(8):138. <https://doi.org/10.3390/computation10080138>.
3. Khalaf AB. Using remote sensing and geographic information systems to study the change detection in temperature and surface area of Hamrin Lake. *Baghdad Sci. j.* 2022;19(5):1130. <https://dx.doi.org/10.21123/bsj.2022.6420>
4. Lan D, Liang B, Bao C, Ma M, Xu Y, Yu C. Marine oil spill risk mapping for accidental pollution and its application in a coastal city. *Mar. Pollut. Bull.* . 2015;96(1):220-5. <https://doi.org/10.1016/j.marpolbul.2015.05.023>
5. Jafari R, Razvarz S, Gegov A, Vatchova B. Deep Learning for Pipeline Damage Detection: an Overview of the Concepts and a Survey of the State-of-the-Art 2020 2020 *IEEE 10th International Conference on Intelligent Systems (IS)*, Varna, Bulgaria, 2020, pp. 178-182. <https://doi.org/10.1109/IS48319.2020.9200137>.
6. Jafarzadeh H, Mahdianpari M, Homayouni S, Mohammadimanesh F, Daboor M. Oil spill detection from Synthetic Aperture Radar Earth observations: a meta-analysis and comprehensive review. *GISci Remote Sens.* . 2021;58(7):1022-51. <https://doi.org/10.1080/15481603.2021.1952542>
7. Jafari R, Razvarz S, Gegov A, Vatchova B, editors. Deep Learning for Pipeline Damage Detection: an Overview of the Concepts and a Survey of the State-of-the-Art. 2020 *IEEE 10th International Conference on Intelligent Systems (IS)*; 2020: IEEE. Varna, Bulgaria. 2020; pp. 178-182. <https://doi.org/10.1109/IS48319.2020.9200137>.
8. Xu J, Wang H, Cui C, Zhao B, Li B. Oil spill monitoring of shipborne radar image features using SVM and local adaptive threshold. *Algorithms.* 2020;13(3):69. <https://doi.org/10.3390/a13030069>.
9. Shaban M, Salim R, Abu Khalifeh H, Khelifi A, Shalaby A, El-Mashad S, et al. A deep-learning framework for the detection of oil spills from SAR data. *Sensors.* 2021;21(7):2351. <https://doi.org/10.3390/s21072351>
10. Huby AA, Sagban R, Alubady R, editors. Oil Spill Detection based on Machine Learning and Deep Learning: A Review. *IICETA 2022 - 5th International Conference on Engineering Technology and its Applications.* 2022; pp. 85-90. <https://doi.org/10.1109/IICETA54559.2022.9888651>.
11. Chhotaray G, Kulshreshtha A, editors. Defect detection in oil and gas pipeline: A machine learning application. *Data Management, Analytics and Innovation: Proceedings of ICDMAI.* 2018; Volume 2: pp. 177-184. https://doi.org/10.1007/978-981-13-1274-8_14.

12. Temitope Yekeen S, Balogun ALL, Wan Yusof KB. A novel deep learning instance segmentation model for automated marine oil spill detection. *ISPRS*. 2020;167:190-200.
<https://doi.org/10.1016/j.isprsjprs.2020.07.011>.
13. Ghorbani Z, Behzadan AH, editors. Identification and instance segmentation of oil spills using deep neural networks. CSEE. 2020: Avestia Publishing.
<https://doi.org/10.11159/iceptp20.140>.
14. Zeng K, Wang Y. A deep convolutional neural network for oil spill detection from spaceborne SAR images. *Remote Sens*. 2020;12(6).
<https://doi.org/10.3390/rs12061015>.
15. Zhao X, Wang X, Du Z, editors. Research on Detection Method for the Leakage of Underwater Pipeline by YOLOv3. 2020 IEEE International Conference on Mechatronics and Automation, ICMA 2020; 2020 2020/10//: Institute of Electrical and Electronics Engineers Inc, Beijing, China. 2020; pp. 637-642.
<https://doi.org/10.1109/ICMA49215.2020.9233693>.
16. Sheta A, Alkasassbeh M, Braik M, Ayyash HA. Detection of oil spills in SAR images using threshold segmentation algorithms. *Int. J. Comput.*2012;57(7).
17. Hu G, Xiao X, editors. Edge detection of oil spill using SAR image. 2013 Cross Strait Quad-Regional Radio Science and Wireless Technology Conference; 2013: IEEE, Chengdu, China.2013;pp. 466-469.
<https://doi.org/10.1109/CSQRWC.2013.6657456>.
18. Li Y, Yang X, Ye Y, Cui L, Jia B, Jiang Z, et al., editors. Detection of oil spill through fully convolutional network. *Geo-Spatial Knowledge and Intelligence: 5th International Conference, GSKI 2017, Chiang Mai, Thailand, December 8-10, 2017, Revised Selected Papers, Part I 5*; 2018. Springer.
https://doi.org/10.1007/978-981-13-0893-2_38.
19. Ghorbani Z, Behzadan AH. Monitoring offshore oil pollution using multi-class convolutional neural networks. *Environ. Pollut.* . 2021;289.
<https://doi.org/10.1016/j.envpol.2021.117884>.
20. Löw F, Stieglitz K, Diemar O. Terrestrial oil spill mapping using satellite earth observation and machine learning: A case study in South Sudan. *J. Environ. Manage.* . 2021;298.
<https://doi.org/10.1016/j.jenvman.2021.113424>.
21. Basit A, Siddique MA, Sarfraz MS, editors. Deep Learning Based Oil Spill Classification Using Unet Convolutional Neural Network. *IGARSS*. 2021; pp. 3491-3494.
<https://doi.org/10.1109/IGARSS47720.2021.955364>.
22. Shaban M, Salim R, Khalifeh HA, Khelifi A, Shalaby A, El-Mashad S, et al. A deep-learning framework for the detection of oil spills from SAR data. *Sensors*. 2021;21(7), 2351.
<https://doi.org/10.3390/s21072351>.
23. Wang X, Liu J, Zhang S, Deng Q, Wang Z, Li Y, et al. Detection of Oil Spill Using SAR Imagery Based on AlexNet Model. *Comput. Intell. Neurosci.* .2021.
<https://doi.org/10.1155/2021/4812979>.
24. Mehta N, Shah P, Gajjar P. Oil spill detection over ocean surface using deep learning: a comparative study. *Mar. Syst. Ocean Technol.* . 2021;16(3-4):213-20. <https://doi.org/10.1007/s40868-021-00109-4>
25. Said M, Hany M, Magdy M, Saleh O, Sayed M, Hassan YM, et al. Automated labeling of hyperspectral images for oil spills classification. *Int. J. Adv. Comput.* 2021;12(8).
<http://dx.doi.org/10.14569/IJACSA.2021.0120857>
26. Asroni A, Ku-Mahamud KR, Damarjati C, Slamet HB. Arabic speech classification method based on padding and deep learning neural network. *Baghdad Sci.J.* 2021;18(2(Suppl.)):0925.
[https://dx.doi.org/10.21123/bsj.2021.18.2\(Suppl.\).0925](https://dx.doi.org/10.21123/bsj.2021.18.2(Suppl.).0925)
27. Topouzelis K, Psyllos A. Oil spill feature selection and classification using decision tree forest on SAR image data. *ISPRS*. 2012;68:135-43.
<https://doi.org/10.1016/j.isprsjprs.2012.01.005>
28. ul Khairi D, Ayaz F, Saeed N, Ahsan K, Ali SZ. Analysis of deep convolutional neural network models for the fine-grained classification of vehicles. *Future Transportation*. 2023;3(1):133-49.
<https://doi.org/10.3390/futuretransp3010009>
29. Adegun AA, Viriri S, Tapamo J-R. Review of deep learning methods for remote sensing satellite images classification: experimental survey and comparative analysis. *J. Big Data*. 2023;10(1):93.
<https://doi.org/10.1186/s40537-023-00772-x>.
30. Kingma DP, Ba J. Adam: A method for stochastic optimization. *arXiv preprint arXiv:1412.6980*. 2014.
<https://doi.org/10.48550/arXiv.1412.6980>.
31. Sharma A, Kodipalli A, Rao T, editors. Performance of Resnet-16 and Inception-V4 Architecture to Identify Covid-19 from X-Ray Images. 2022 IEEE 9th Uttar Pradesh Section International Conference on Electrical, Electronics and Computer Engineering (UPCON); 2022 2-4 Dec. 2022. Prayagraj, India, 2022, pp. 1-6.
<https://doi.org/10.1109/UPCON56432.2022.9986372>.
32. Simonyan K, Zisserman A. Very deep convolutional networks for large-scale image recognition. *arXiv preprint arXiv:1409.1556*. 2014.
<https://doi.org/10.48550/arXiv.1409.1556>.

تصنيف الانسكابات النفطية على أساس الصور الفضائية باستخدام تقنيات التعلم العميق

أبو بكر صالحو أبا، نورفا هاسلينا مصطفى، ستي زيتون محمد هاشم، رزاة علوي

كلية الحاسبات، الجامعة التكنولوجية، جوهور باهرو، ماليزيا.

الخلاصة

التسرب النفطي هو تسرب في خطوط الأنابيب أو السفن أو منصات النفط أو الناقلات يؤدي إلى انطلاق المنتجات البترولية في البيئة البحرية أو على اليابسة بشكل طبيعي أو بسبب عمل بشري، مما يؤدي إلى أضرار جسيمة وخسائر مالية. تعد صور الأقمار الصناعية إحدى الأدوات القوية المستخدمة حالياً لالتقاط المعلومات الحيوية والحصول عليها من سطح الأرض. لكن التعقيد والكم الهائل من البيانات يجعل من الصعب على البشر معالجتها ويستغرق وقتاً طويلاً. ومع ذلك، مع تقدم تقنيات التعلم العميق، أصبحت العمليات الآن محوسبة للعثور على المعلومات الحيوية باستخدام صور الأقمار الصناعية في الوقت الحقيقي. طبقت هذه الورقة ثلاث خوارزميات للتعلم العميق لتصنيف صور الأقمار الصناعية، بما في ذلك ResNet50، وVGG19، وInceptionV4؛ تم تدريبهم واختبارهم على مجموعة بيانات صور الأقمار الصناعية مفتوحة المصدر لتحليل كفاءة الخوارزميات وأدائها وربط دقة التصنيف والدقة والاستدعاء ودرجة f1. وأظهرت النتيجة أن InceptionV4 يعطي أفضل دقة تصنيف بنسبة 97% للغيوم والصحراوية والمناطق الخضراء والمياه، يليه VGG19 بنسبة 96% تقريباً وResNet50 بنسبة 93%. أثبتت النتائج أن خوارزمية InceptionV4 مناسبة لتصنيف الانسكابات النفطية وعدم الانسكابات باستخدام صور الأقمار الصناعية على مجموعة بيانات تم التحقق من صحتها.

الكلمات المفتاحية: التصنيف، البحرية، التسرب النفطي، صور الأقمار الصناعية، التعلم العميق.